Extended detrended fluctuation analysis of electroencephalograms signals during sleep and the opening of the blood–brain barrier

Cite as: Chaos **30**, 073138 (2020); https://doi.org/10.1063/5.0011823
Submitted: 24 April 2020 . Accepted: 07 July 2020 . Published Online: 24 July 2020

A. N. Pavlov, A. I. Dubrovsky, A. A. Koronovskii, O. N. Pavlova, O. V. Semyachkina-Glushkovskaya, and J. Kurths

Extended detrended fluctuation analysis of electroencephalograms signals during sleep and the opening of the blood–brain barrier

Cite as: Chaos **30**, 073138 (2020); doi: 10.1063/5.0011823
Submitted: 24 April 2020 · Accepted: 7 July 2020 ·
Published Online: 24 July 2020

A. N. Pavlov,[1,a)] A. I. Dubrovsky,[2] A. A. Koronovskii, Jr.,[1] O. N. Pavlova,[2] O. V. Semyachkina-Glushkovskaya,[3] and J. Kurths[3,4,5]

AFFILIATIONS

[1]Department of Nonlinear Processes, Saratov State University, Astrakhanskaya Str. 83, 410012 Saratov, Russia
[2]Department of Physics, Saratov State University, Astrakhanskaya Str. 83, 410012 Saratov, Russia
[3]Deparatment of Biology, Saratov State University, Astrakhanskaya Str. 83, 410012 Saratov, Russia
[4]Potsdam Institute for Climate Impact Research, Telegraphenberg A 31, 14473 Potsdam, Germany
[5]Institute of Physics, Humboldt University Berlin, 12489 Berlin, Germany

[a)]**Author to whom correspondence should be addressed:** pavlov.alexeyn@gmail.com

ABSTRACT

Detrended fluctuation analysis (DFA) is widely used to characterize long-range power-law correlations in complex signals. However, it has restrictions when nonstationarity is not limited only to slow variations in the mean value. To improve the characterization of inhomogeneous datasets, we have proposed the extended DFA (EDFA), which is a modification of the conventional method that evaluates an additional scaling exponent to take into account the features of time-varying nonstationary behavior. Based on EDFA, here, we analyze rat electroencephalograms to identify specific changes in the slow-wave dynamics of brain electrical activity associated with two different conditions, such as the opening of the blood–brain barrier and sleep, which are both characterized by the activation of the brain drainage function. We show that these conditions cause a similar reduction in the scaling exponents of EDFA. Such a similarity may represent an informative marker of fluid homeostasis of the central nervous system.

Natural systems often exhibit complex dynamics with long-range power-law correlations. To quantify this phenomenon, different variants of fluctuation analysis are used with detrended fluctuation analysis (DFA),[1,2] representing a universal method that can be applied to both stationary and nonstationary time series. In many practical situations, however, nonstationarity cannot be eliminated by simply removing the slow variation in mean value. For such a case, we have recently proposed an extended method (EDFA), which estimates two scaling exponents: the first exponent is associated with the conventional DFA and the second exponent quantifies the impact of nonstationarity.[3] Here, we use EDFA to identify informative markers of changes in electroencephalograms associated with two different factors, namely, open blood–brain barrier (BBB) and sleep, which are characterized by activated brain drainage function. By means of EDFA, we uncover that both factors, sound and sleep, cause similar changes in the low-frequency dynamics of electroencephalograms (EEG). These results offer a hint of the similarity of EEG dynamics related to distinct mechanisms of fluid drainage from the brain during sleep and after the BBB opening.

I. INTRODUCTION

Complex dynamics with long-range correlations are typical for many natural systems.[4] The processes created by such systems often exhibit power-law statistics, and their characterization is widely used to identify structural changes which occur as a result of variations in external conditions or transitions between different types of system behavior. For stationary processes, the correlation function or spectral power is mainly applied, which are interrelated in accordance to the Wiener–Khinchin theorem.[5,6] Nevertheless, the analysis of long-range correlations in experimental data is limited even for systems with stable parameters due to the rapidly decreasing correlation

function for stochastic/chaotic time series. To avoid significant errors in the computing of scaling characteristics in the range where this function approaches zero, a method based on random walk analysis was proposed,[1,2] which introduces a growing dependence, whose scaling exponent is easy to estimate. This method, called detrended fluctuation analysis (DFA), has become a universal signal processing tool, especially when studying complex systems with time-varying parameters.[7–16] It involves a trend removal procedure, i.e., excluding of slow nonstationarity from time series, which allows DFA to be applied to experimental data without their preliminary processing. In this regard, DFA is similar to another popular method, namely, the continuous wavelet transform[17] that does not require detrending if wavelets with several vanishing moments are applied, and a polynomial trend of the corresponding order is automatically ignored. Despite existing discussions about the limitations of DFA,[18–21] this tool has been often used because of its simplicity and effectiveness in characterizing long-range correlations.

It is important to note that the DFA deals with one basic type of nonstationarity consisting of slow variations in the local mean value. However, the time-varying dynamics of natural systems often includes a wider range of complex phenomena responsible for nonstationary behavior, e.g., (i) the variability of trend characteristics throughout the signal, when the degree of nonstationarity changes significantly for individual data segments; (ii) time-varying dynamics in higher frequency ranges compared to slow oscillations being excluded due to the detrending procedure; and (iii) nonstationarity in energy that is not taken into account in the DFA. These circumstances are the reason for possible improvements of this popular tool aimed at expanding its capabilities in characterizing the complex dynamics from the acquired time series. A way of such improvement is a multifractal DFA[22] that evaluates a number of numerical measures for deeper understanding the complex organization of inhomogeneous datasets. In our recent study,[3] we have proposed another modification of the conventional method DFA, called extended DFA (EDFA). In addition to a single scaling exponent (in the case of its global assessment), which quantifies the long-range correlations, we suggested to take into account the impact of nonstationarity. The latter often changes throughout the signal and is described by another scaling exponent being sensitive not only to slow variations in the local mean value but also to other types of nonstationary behavior. Both of these exponents are useful as diagnostic measures in experimental studies.[3]

In this paper, we demonstrate the potential of EDFA in studying the electrical activity of the brain in rats. For this purpose, we consider an important problem in the diagnostics of low-frequency changes, which can occur upon the activation of brain drainage function during sleep or after the opening of the blood–brain barrier.[23–25] This problem has attracted considerable attention over the past decade in connection with the delivery of drugs to the brain being one of the basic problems in neuroscience.[26–28] There is an intensive growing body of evidence that sleep and lymphatics play a crucial role in keeping the health of the central nervous system (CNS) via the night activation of drainage of brain tissues and clearance of metabolites and neurotoxins.[29–34] Sleep can be the natural factor for the activation of the cerebral lymphatics. Indeed, Xie *et al.*[30] discovered that sleep is associated with increased clearance of metabolic waste products. However, it is unknown why these processes co-occur and how they are related. Fultz *et al.*[29] discovered the activation of oscillations of brain fluids with specific slow-wave pattern of electrophysiological changes during deep sleep. These results demonstrate that the sleeping brain exhibits waves of brain fluid flow on a macroscopic scale. In our previous animal data, we uncovered activation of clearing function of the cerebral lymphatics after opening of the BBB associated with changes in fluid homeostasis in the brain.[32,33] The BBB plays a crucial role in keeping the health of CNS forbidding penetration into the brain bacterias, viruses, and toxins. The BBB opening immediately activates the cerebral lymphatics to keep the homeostasis of CNS via cleaning of the brain tissues from molecules crossing BBB.[32–34] The ability to stimulate the lymph flow in the sleeping brain is likely to play an important role in developing innovative methods in neurorehabilitation therapy. However, there is no effective and non-invasive methods for real-time monitoring and analysis of drainage and clearing functions of the cerebral lymphatics that significantly slows down progress in the appearance of technologies for therapeutic modulations of the lymphatics in the CNS.

The BBB opening with a further recovery of its protective function can be caused, e.g., by sound when using loud music or intermittent sound for 2 h. The effect of sound on the BBB permeability was verified by many experimental techniques: magnetic resonance imaging, two-photon microscopy, fluorescence analysis, spectrofluorimetric and confocal analysis, and the results of histological analysis.[32–34] Some of these methods are used within *in vivo* studies but they require expensive equipment or invasive procedures. That is why the question arises whether it is possible to detect related changes in BBB permeability using only non-invasive methods such as EEG. We compare here the electrical activity of the brain in awake animals during the BBB opening and during sleep. Although the EEG itself does not provide reliable identification of the BBB opening, which should also be confirmed by optical imaging tools, this simple experimental technique could reveal informative markers of changes in the brain dynamics accompanying an activation of the lymphatic drainage function. We will apply here EDFA to uncover such markers. The manuscript is organized as follows. In Sec. II, we briefly describe experiments in rats based on a model of sound-induced reversible BBB opening and compare the effects of sound and sleep on the long-range correlations in EEG dynamics. Besides, this section contains a general description of the extended DFA method used for signal processing. Our main results describing changes in EEG recordings are presented in Sec. III. Section IV summarizes the conclusions of this study.

II. MATERIALS AND METHODS

The experiments described in this section include two stages: preliminary experiments to confirm the BBB opening (stage 1) and experiments with EEG records used to reveal informative markers of changes in brain dynamics (the main goal of this study, stage 2).

A. Stage 1: Sound-induced BBB opening

These preliminary experiments were carried out in four groups: (1) without sound—control group and (2)–(4)—1, 4, and 24 h after sound exposure in freely moving rats, respectively (n = 10 in

each group). To produce a loud sound (100 dB, 370 Hz), a sound speaker was used (7 A, 12 V, Auto VAZ PJSC, Tolyatti, Russia). The intermittent sound exposure was applied for 2 h in accordance with a repeating procedure: 1 min of sound and 1 min pause.

A fluorescence microscope was used to *in vivo* visualize extravasation of albumin complex of Evans blue dye (EBAC, 2 mg/25 g mouse, 1% solution in saline, iv) via an optically cleaned skull window in anesthetized rats (2% isoflurane at 1 l/min N_2O/O_2—70:30).[35] Images were recorded immediately and 30 min after administration of EBAC to rats with open BBB. For *ex vivo* analysis of EBAC leakage, spectrofluorimetric assay was used.[36] Three days before the experiments, a polyethylene catheter was implanted into the femoral vein for intravenous injection of Evans blue dye in awake animals. Before or 1 h/4 h/24 h after sound exposure, Evans blue dye was injected and circulated in the blood for 30 min in accordance with the recommended protocol.[36] At the end of the circulation time, rats were decapitated, their brains were quickly collected and placed on ice (no anti-coagulation was used during blood collection). Before removing the brain, it was perfused with saline to wash out the remaining dye in the cerebral vessels. A detailed protocol for the isolation and visualization of the Evans blue albumin complex is described by Wang and Lai.[36]

Fluorescein isothiocyanate-dextran (FITCD) 70 kDa was used as an additional valuable tool for characterizing the BBB permeability to high molecular weight molecules in ten rats. The BBB permeability to FITCD was evaluated *in vitro* by confocal microscopy. The protocol for FITCD to assess the BBB disruption using confocal microscopy is described in details by Hoffmann *et al.*[37] Briefly, before or 1, 4, and 24 h after sound exposure, FITCD 70 kDa (1 mg/25 g mouse, 0.5% solution in saline, Sigma-Aldrich) was injected into the tail vein and allowed to circulate for 2 min. Afterward, the brain was fixed with 4% neutral buffered formalin. After fixation, the brain was cryoprotected using 20% sucrose in phosphate buffered saline (PBS) (10 ml/brain mouse) for 48 h at 4°C. The brain was frozen in hexane cooled to −36°C. Cryosections (14 μm) of parietal cortex were collected on poly-L-Lys, polysine slides (Menzel-Glaser, Germany) using a cryotome (Thermo Scientific Microm HM 525, Germany) and a liquid for fixing a tissue-tek sample (Sakura Finetek, USA). Cryosections were blocked in 150 μl 10% BSA/PBS for 1 h and then incubated overnight at 4 °C with 130 μl of goat anti-mouse NG2 antibody (1:500; ab 50009, Abcam, Cambridge, United Kingdom) and rabbit antibodies (1:500, clone EPR19996, Elisa, USA) to rat glial fibrillary acidic protein (GFAP). After several rinses in PBS, the slides were incubated for 1 h with 130 μl of fluorescent-labeled secondary antibodies [goat anti-mouse IgG (H+L) Alexa Flour 647 and 405; Invitrogen, Molecular Probes, Eugene, Oregon, USA]. The confocal microscopy was performed using a Nikon TE 2000 Eclipse microscope, Tokyo, Japan. Approximately 8–12 slices per animal from the cortical and subcortical regions were imaged (excluding the hypothalamus and choroid plexus, where the BBB is leaky).

B. Stage 2: EEG measurements

The experiments were carried out on nine adult male Wistar rats (250–280 g) in accordance with the Guide for the Care and Use of Laboratory Animals (8th ed. The National Academies Press, Washington, 2011). The protocols were approved by the local ethics committee at the Saratov State University. The animals were kept in a light/dark environment with the lights on from 8:00 to 20:00 and fed *ad libitum* with standard rodent food and water. Ambient temperature and humidity were maintained between 22 and 24 °C and 40%–60%, respectively.

A two-channel cortical EEG/one channel electromyogram (EMG) (Pinnacle Technology, Taiwan) were recorded using electrodes (tip diameter 2–3 μm) located at a depth of 150 μm in coordinates (L: 2.5 mm and D: 2 mm) from Bregma. EEG activity was measured and compared in awake and sleeping rats. Wake/sleep states were scored in 4 s epochs. Wakefulness was defined as a desynchronized EEG with low amplitude and high-frequency dynamics (>10% waveforms of >12 Hz) and relatively high-amplitude EMG. A state of non-rapid eye movement (NREM) sleep was recognized as synchronized activity with high amplitude, which is dominated by low-frequency delta waves (0–4 Hz) comprising >30% of EEG waveforms/epoch and a lower amplitude EMG. REM was identified by the presence of theta waves (5–10 Hz) comprising >20% of EEG waveforms/epoch with a low EMG amplitude. Each epoch included in the analyses of sleep/wake studies was visually checked. EEG recording was carried out on the same rats under different conditions.

In our study, three states are considered: (1) awake rats with closed BBB (control state), (2) awake rats with open BBB (1 h after sound exposure), and (3) sleeping animals. All measurements were done with a sampling frequency of 2 kHz. The removal of movement artifacts was performed using the method of wavelet enhanced independent component analysis.[38] Despite the fact that any approach does not guarantee that artifacts will be completely removed (as a rule, their effect is reduced), for states (1) and (2) in awake rats, we chose 10-min segments of records (for each EEG-channel) with a fairly homogeneous structure. The latter was controlled by a floating window analysis that included DFA for 1-min parts and selection of segments with minimal standard deviation of the scaling exponents. For the sleep state, we used 10-min segments of NREM sleep, also providing an analogous selection of fragments using an automatic method. Results for both channels were averaged for each rat.

C. Detrended fluctuation analysis (DFA)

DFA, originally proposed by Peng *et al.*,[1,2] is a variant of the root mean square (RMS) analysis of random walks, which provides fitting and extraction of a local trend. Its algorithm involves integrating a time series $x(i)$ of length N with a subtracted mean value

$$y(k) = \sum_{i=1}^{k} [x(i) - \langle x \rangle], \quad \langle x \rangle = \sum_{i=1}^{N} x(i). \tag{1}$$

Furthermore, the resulting profile or random walk $y(k)$ is divided into non-overlapping segments of equal length n. Within each segment, the local trend $y_n(k)$ is estimated in accordance with the least squares approach. A linear fit is usually performed, although other functions (e.g., polynomials) may also be applied. At the next stage, the standard deviation of the signal profile around the

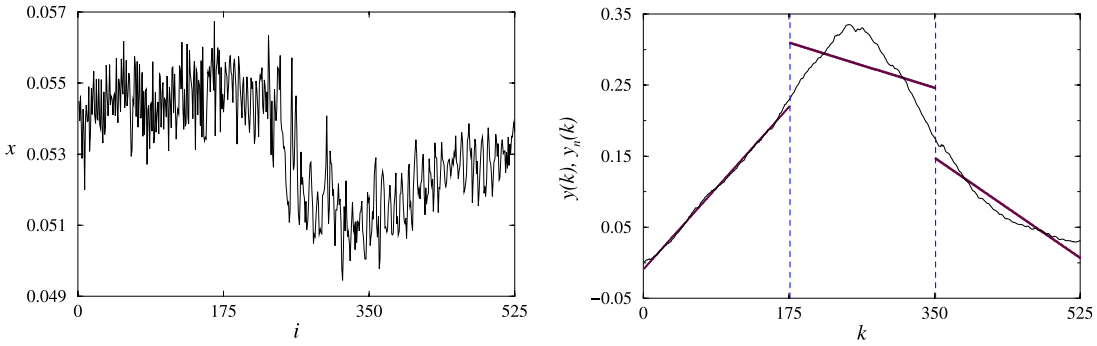

FIG. 1. An example of a nonstationary signal (changes in the mean value) (a) and its random walk with a piece-wise linear fitting (b). There is a clear difference in the local standard deviations of $y(k)$ from $y_n(k)$ which is shown by a bold piece-wise linear function.

local trend is computed,

$$F(n) = \sqrt{\frac{1}{N}\sum_{k=1}^{N}[y(k) - y_n(k)]^2}, \tag{2}$$

and such an algorithm is applied for different segment sizes (n) to obtain the dependence $F(n)$ over a wide range of scales. Typically, $F(n)$ is a growing dependency, and its power-law behavior,

$$F(n) \sim n^{\alpha}, \tag{3}$$

indicates the presence of scaling, characterized by the α-exponent that is easily evaluated on a log–log plot. This exponent reflects various types of correlated and uncorrelated behavior of the time series $x(i)$, in particular, anti-correlations associated with alternating small and large values of the signal $x(i)$ ($\alpha < 1/2$), the absence of correlations related to white noise ($\alpha = 1/2$), power-law positive correlations ($1/2 < \alpha < 1$), and positive correlations that cease to demonstrate a power-law behavior ($\alpha > 1$). Note that the exponent α is related to the quantities describing the decay of the correlation function or spectral power.[1]

D. Extended detrended fluctuation analysis (EDFA)

The inhomogeneous structure of many experimental time series can lead to a strong variability of the RMS fluctuations of the signal profile around the local trend between different segments. Two variants of such variabilities are shown in Figs. 1 and 2 and include the case of a transient process with a changing mean value [Fig. 1(a)] and intermittent dynamics, where the local mean value is nearly constant but the correlation properties of the data segments change [Fig. 2(a)].

Even a visual analysis of the profiles [Figs. 1(b) and 2(b)] makes it clear that the standard deviations of the random walk $y(k)$ from the local trend $y_n(k)$ differ significantly among the data segments. Consequently, some segments will have the strongest effect on the

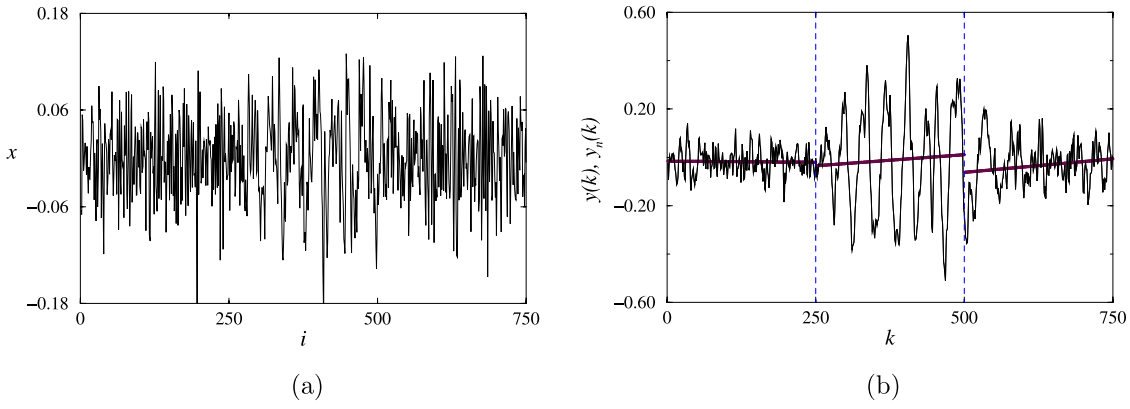

FIG. 2. Another example of a nonstationary signal (intermittent behavior) (a) and the related random walk (b).

values $F(n)$, while the role of other parts of the data becomes quite small. Similar distinctions are observed for other types of signals. To take into account such typical heterogeneity of the RMS fluctuations, we have proposed the following extension of the standard DFA method. In addition to the conventional algorithm, we evaluate a measure,

$$dF(n) = \max\left[F_{loc}(n)\right] - \min\left[F_{loc}(n)\right], \quad (4)$$

describing the impact of nonstationarity,[3] with $F_{loc}(n)$ being the local RMS fluctuations of the signal profile $y(k)$ from the trend $y_n(k)$. Each value of $F_{loc}(n)$ is computed within one segment of length n, i.e., the number of such quantities depends on n. $dF(n)$ is the difference between the maximum and minimum local RMS fluctuations. For a stationary signal with a homogeneous structure, there is a narrow distribution of $F_{loc}(n)$, and the difference $dF(n)$ is small. Otherwise, it can take large values, approaching $\max\left[F_{loc}(n)\right]$. By analogy with $F(n)$, the difference $dF(n)$ usually changes with n and can show a power-law dependence but the latter is described by another scaling exponent,

$$dF(n) \sim n^{\beta}. \quad (5)$$

Figure 3 illustrates different scaling behavior of simulated datasets described by the quantities α and β. Usually, $\beta < \alpha$, and the exponent of the EDFA method (β) can take even negative values [Fig. 3(b)]. The analysis of experimental data[3] also showed that the exponents α and β give different characteristics of the signal structure but do not have a clear relationship with each other. Both of these quantities provide informative measures of the complex organization of datasets. Thus, β characterizes the inhomogeneity of nonstationary behavior throughout the signal. Higher inhomogeneity leads to larger values of β.

III. RESULTS AND DISCUSSION

At the first stage, we studied the effect of loud sound on BBB permeability to EBAC and FITCD using *in vivo* and *ex vivo* experiments. Based on *in vivo* real-time fluorescence microscopy, we observed a significant leakage of EBAC 1 h after sound exposure. Afterward, the brains of the same rats were collected for spectrofluorimetric assay and quantitative analysis of the integrity of BBB. The results of *ex vivo* study showed that the level of EBAC in brain tissues increased by 23.7 times compared with the control group (2.61 ± 0.07 vs 0.11 ± 0.03, $p<0.001$). There were no significant changes in the level of EBAC in brain tissues 4 h and 24 h after sound exposure (0.10 ± 0.05 and 0.13 ± 0.07 compared to 0.11 ± 0.03, respectively). In the normal state, due to the high molecular weight of EBAC (68.5 kDa), it cannot penetrate through an intact BBB, and its leakage into the brain parenchyma indicates a disruption of the BBB.[39,40] Thus, these results allowed us to determine that the BBB opens up to 1 h and closes from 1 h to 4 h after sound exposure (a more accurate BBB closing time requires additional experiments).

For a qualitative assessment of BBB permeability, we used confocal imaging of FITCD leakage. Figure 4 clearly illustrates the extravasation of FITCD from cerebral capillaries into brain tissue 1 h after sound exposure. Note that we did not find increased BBB permeability to FITCD and EBAC 4 h and 24 h after sound exposure.

At the second stage, we considered EEG data in different conditions. Before studying the intergroup distinctions in the electrical activity of the brain, we analyzed how the EEG properties depend on the position of the electrode (on the left or on the right side of the head). This analysis established that the estimated dependencies $F(n)$ and $dF(n)$ in a double logarithmic plot show fairly similar behavior for both records measured in each rat. The scaling characteristics are usually different for relatively short-range correlations ($\lg n < 2.5$, which is associated with frequencies exceeding 6 Hz) and for long-range correlations ($\lg n > 3.3$, which is related to frequencies <1 Hz). The scaling exponents in the middle range ($2.5 < \lg n < 3.3$) usually take intermediate values. Despite of these distinctions, confirming the inhomogeneous structure of the EEG recordings, we find that the results are slightly dependent on the choice of the electrode, and the observed differences are compared with computing errors due to data processing. The latter is observed for both exponents.

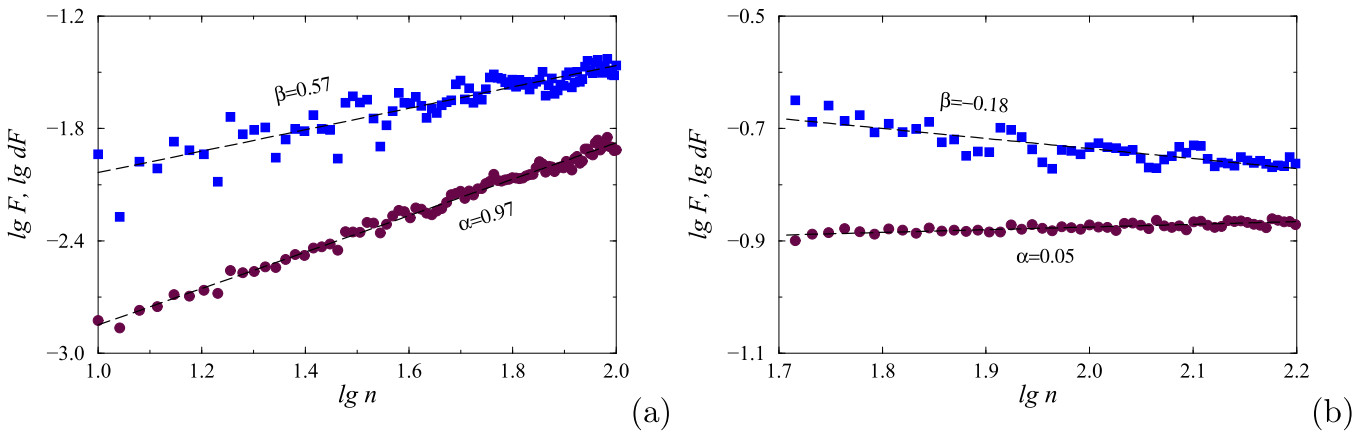

FIG. 3. The dependencies $F(n)$ and $dF(n)$ in the double logarithmic for the time series shown in Fig. 1(a) (a) and Fig. 2(a) (b) exhibit different power-law behavior described by the scaling exponents α and β.

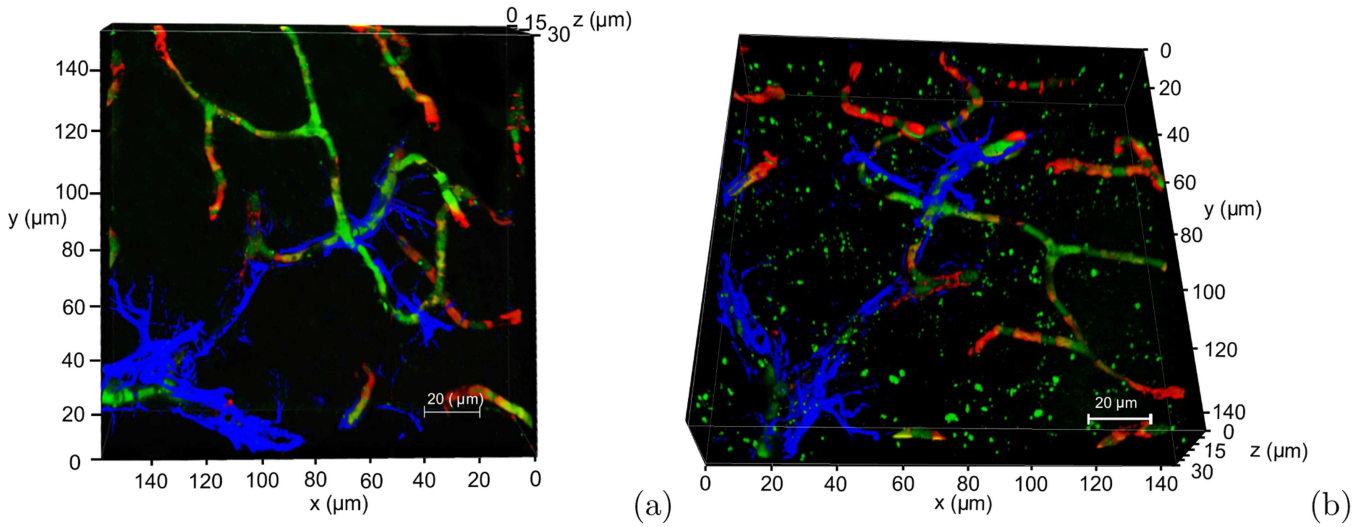

FIG. 4. 3D confocal analysis of BBB permeability to FITCD (green) before (a) and 1 h after (b) sound exposure. Before sound influence, FITCD is located inside the cerebral microvessels (labeled NG2—pericyte marker, red); 1 h after sound exposure FITCD leaks from the cerebral vessels into the brain tissue and its distribution among astrocytes (labeled by GFAP, blue) is observed.

Let us now consider how the BBB opening by sound affects the dynamics of the EEG. Figure 5 illustrates the dependencies for awake rats with closed and open BBB. According to this figure, the main distinctions arise in the region of slow-wave dynamics <1 Hz that is related to long-range correlations in the EEG data and includes a reduction in the α-exponent describing the correlation features of datasets. No significant reactions are revealed in the range $\lg n < 3.3$ that is why we shall further consider frequencies <1 Hz. The values of α are reduced from 0.65 ± 0.04 to 0.47 ± 0.06, which characterize the transition from positive power-law correlations to anti-correlations. Such distinctions ($p < 0.05$ according to the Mann–Whitney test) are clearly detected by the scaling characteristics of conventional DFA. The extended approach (EDFA) demonstrates even clearer differences between both datasets [Fig. 5(b)]. Again, the range of long-range correlations is the most informative from the viewpoint of detecting structural changes in the electrical activity of the brain due to the sound-induced BBB opening. The β-exponent decreases from 0.41 ± 0.05 to 0.07 ± 0.10 ($p < 0.01$, the Mann–Whitney test), i.e., it can take both positive and negative values in an open BBB state. The transition from a positive to a negative value does not always occur but a reduction of the β-exponent is a typical phenomenon. The region of the slow-wave dynamics

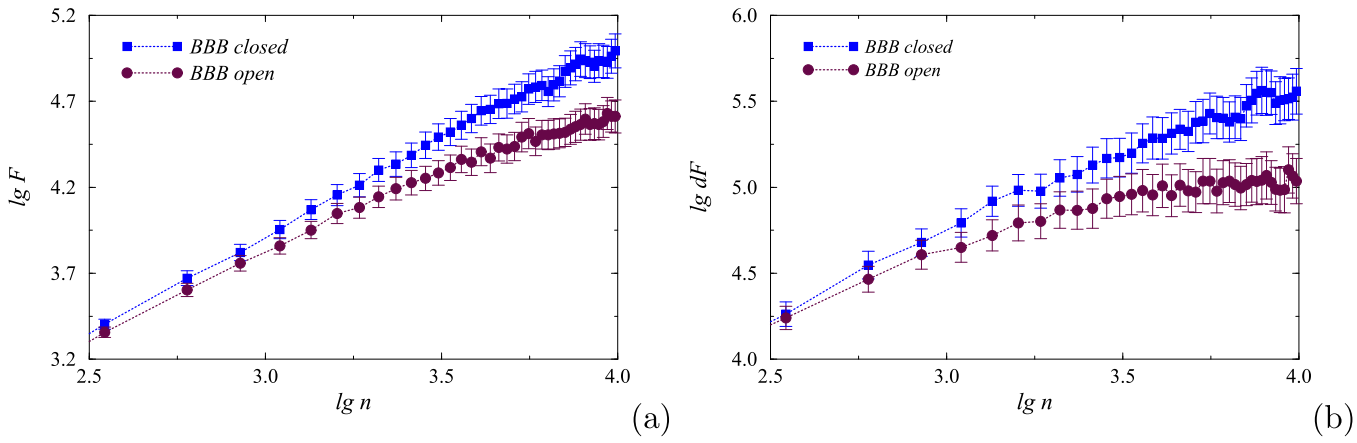

FIG. 5. Reduction of scaling exponents α (a) and β (b) in awake rats with sound-induced activation of brain lymphatic drainage function compared to background measurements (mean±SE).

(<1 Hz) is the most informative for diagnostic studies, when EEG can offer markers indicating the effects of the activated lymphatic drainage function. It is clear that EEG alone cannot confirm that associated changes appear due to this activation and not for any other reason. In order to do this confirmation, an additional experimental technique based on optical imaging should be applied. However, the preliminary detection of structural changes in the experimental data can be achieved using EEG.

Note that a similar decrease in scaling characteristics occurs during NREM sleep, and the observed intergroup distinctions are similar to the case of sound-induced BBB opening. Figure 6 shows differences between characteristics of EEG signals in awake rats and rats during sleep. Here, the β-exponent is reduced from 0.41 ± 0.05 to 0.14 ± 0.12, which is a strong distinction ($p < 0.01$, the Mann–Whitney test). Such differences confirm that sleep also can alter the long-range correlations in the structure of experimental records. These changes may be related to activated lymphatic drainage function that is in accordance with physiological assumptions. However, as in the previous example, we cannot prove the mechanisms responsible for the observed distinctions based only on EEG recordings. This means that EEG as a simple and non-expensive technique is suitable for detecting structural changes in experimental data, which (as we suppose and as was earlier shown by other experimental tools) may be the consequence of activated lymphatic drainage function. However, a rigorous confirmation is necessary to do during experiments with simultaneous measurements, e.g., EEG and MRI. The latter requires a more complex experimental design but it can further be provided in order to establish physiological interpretation of mechanisms responsible for the revealed changes.

Figures 5 and 6 show statistical results of EDFA analysis, where differences in EEG dynamics are identified. Figure 7 gives the results for individual animals. This figure confirms the main findings of the performed study. A reduction of α and β-exponents in the state of open BBB (squares) compared with the background EEG in awake rats when BBB is closed (circles) is observed. This reduction

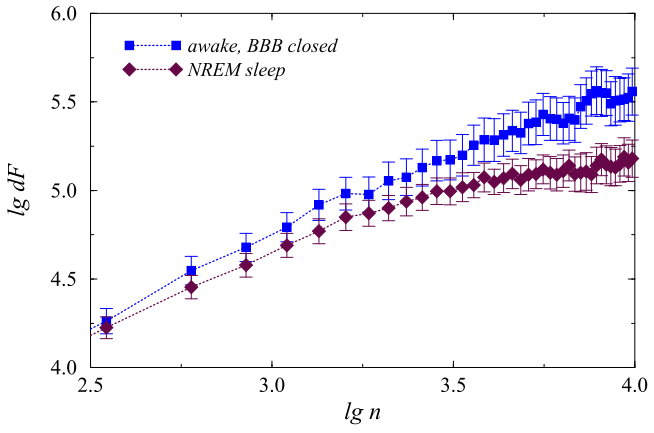

FIG. 6. Reduction of the scaling exponents β during NREM sleep compared to background EEG in awake rats.

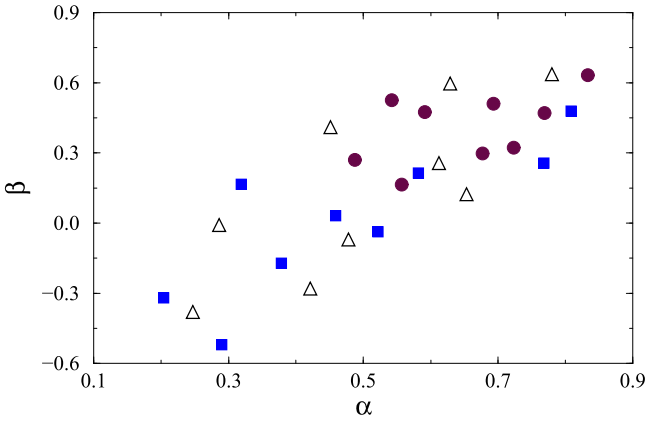

FIG. 7. Scaling exponents estimated for all animals in different states: awake rats with closed BBB (circles), awake rats with open BBB (squares), and during sleep (triangles).

occurs in seven out of nine rats. In general, each of the scaling exponents can be applied to identify these changes but their simultaneous application gives a clearer visualization of the results (Fig. 7). A reduction of scaling exponents is also observed for sleep data compared to the background electrical activity of the brain in the waking state. The changes in mean (over group) values are smaller compared to sound-induced BBB opening.

Thus, in this paper, we illustrated the potential of EDFA in studying changes in the structure of EEG data caused by changes in the state of the body (sleep and sound). The extension of the conventional fluctuation analysis provides better opportunities compared to DFA for characterizing the complex organization of EEG signals, which can be used for diagnostics. Note that the EDFA characterizes the increased slow-wave activity, which is consistent with both NREM deep sleep and lymphatic drainage. Typically, such changes can be detected with the power density analysis, commonly used in physiological studies. The advantage of fluctuation analysis is the ability to better reveal the scaling features in experimental data in the range of very low frequencies (long-range correlations). In particular, the correlation function approaches zero in this region for stochastic/chaotic processes, and the presence of experimental noise complicates the estimates. In contrast, DFA-based approaches are less suitable for studying high-frequency dynamics, where traditional spectral and correlation analyses may be preferred.

IV. CONCLUSION

We examined the possibilities of detrended fluctuation analysis and its extended version, EDFA, in studying the effects of long-range correlations in electrical brain activity in rats. DFA is a useful method for correlation analysis of nonstationary data, which eliminates the scaling exponent α having a relation to exponents describing the decay of the correlation function or spectral power. The proposed extended DFA introduces an additional quantity β that changes depending on the inhomogeneity of the time-varying

dynamics. For fairly homogeneous processes, when the nonstationarity does not essentially vary throughout the signal, this quantity approaches zero and shows a subtle dependence on the length of segments. For inhomogeneous datasets, where the distribution of local standard deviations of the signal profile around the local trend becomes much wider, β enables us to separate processes with different nonstationary behavior.

Unlike many other studies of EEG recordings, here we focus on slow-wave dynamics (<1 Hz), i.e., at frequencies below the rhythms that are usually investigated. The considered frequency range is influenced by slow nonstationarities but their features are different for the background electrical activity of the brain and for the state when the permeability of the blood–brain barrier increases. Two cases are discussed: 2-h sound and NREM sleep. In the first case, a significant reduction in both exponents is observed, and their simultaneous consideration improves the separation between groups, providing a clearer clustering on the (α, β) plane. Intergroup distinctions are confirmed by the Mann–Whitney test ($p < 0.05$ for both quantities). Although such changes cannot be directly related to the lymphatic drainage function, the results of additional studies with optical imaging approaches verify that the considered sound affects the BBB permeability. Based on these experimental techniques, we can argue about the markers of such increased permeabilities computed from EEG records. Further studies in this area can expand current knowledges of the available mechanisms of drug transfer to the brain. Similarly, although there is sometimes a lesser decrease in scaling exponents during sleep, this effect is also important in understanding how lymphatic drainage function can be activated. The latter result offers a further question about the role of the sleep stage on this function, which, in our opinion, is an important area of future research.

ACKNOWLEDGMENTS

This work was supported by the RF Government (Grant No. 075-15-2019-1885). A.N.P. acknowledges support by the grant of the President of the Russian Federation for leading scientific schools (No. NSh-2594.2020.2) and by the Mathematical Center of the Saratov State University. We thank the anonymous reviewers whose comments/suggestions helped improve and clarify this manuscript.

DATA AVAILABILITY

The data that support the findings of this study are available from the corresponding author upon reasonable request.

REFERENCES

[1]C.-K. Peng, S. V. Buldyrev, S. Havlin, M. Simons, H. E. Stanley, and A. L. Goldberger, "Mosaic organization of DNA nucleotides," Phys. Rev. E **49**, 1685–1689 (1994).
[2]C.-K. Peng, S. Havlin, H. E. Stanley, and A. L. Goldberger, "Quantification of scaling exponents and crossover phenomena in nonstationary heartbeat time series," Chaos **5**, 82–87 (1995).
[3]A. N. Pavlov, A. S. Abdurashitov, A. A. Koronovskii, Jr., O. N. Pavlova, O. V. Semyachkina-Glushkovskaya, and J. Kurths, "Detrended fluctuation analysis of cerebrovascular responses to abrupt changes in peripheral arterial pressure in rats," Commun. Nonlinear Sci. Numer. Simulat. **85**, 105232 (2020).
[4]D. Sornette, *Critical Phenomena in Natural Sciences*, 2nd ed. (Springer, Berlin, 2004).
[5]N. Wiener, "Generalized harmonic analysis," Acta Math. **55**, 117–258 (1930).
[6]A. Khintchine, "Korrelationstheorie der stationären stochastischen prozesse," Math. Ann. **109**, 604–615 (1934).
[7]H. E. Stanley, L. A. N. Amaral, A. L. Goldberger, S. Havlin, P. C. Ivanov, and C.-K. Peng, "Statistical physics and physiology: Monofractal and multifractal approaches," Physica A **270**, 309–324 (1999).
[8]K. Ivanova and M. Ausloos, "Application of the detrended fluctuation analysis (DFA) method for describing cloud breaking," Physica A **274**, 349–354 (1999).
[9]P. Talkner and R. O. Weber, "Power spectrum and detrended fluctuation analysis: Application to daily temperatures," Phys. Rev. E **62**, 150–160 (2000).
[10]C. Heneghan and G. McDarby, "Establishing the relation between detrended fluctuation analysis and power spectral density analysis for stochastic processes," Phys. Rev. E **62**, 6103–6110 (2000).
[11]J. W. Kantelhardt, E. Koscielny-Bunde, H. H. A. Rego, S. Havlin, and A. Bunde, "Detecting long-range correlations with detrended fluctuation analysis," Physica A **295**, 441–454 (2001).
[12]Q. D. Y. Ma, R. P. Bartsch, P. Bernaola-Galván, M. Yoneyama, and P. C. Ivanov, "Effect of extreme data loss on long-range correlated and anticorrelated signals quantified by detrended fluctuation analysis," Phys. Rev. E **81**, 031101 (2010).
[13]D. Horvatic, H. E. Stanley, and B. Podobnik, "Detrended cross-correlation analysis for non-stationary time series with periodic trends," Europhys. Lett. **94**, 18007 (2011).
[14]O. N. Pavlova, A. S. Abdurashitov, M. V. Ulanova, N. A. Shushunova, and A. N. Pavlov, "Effects of missing data on characterization of complex dynamics from time series," Commun. Nonlinear Sci. Numer. Simulat. **66**, 31–40 (2019).
[15]N. S. Frolov, V. V. Grubov, V. A. Maksimenko, A. Lüttjohann, V. V. Makarov, A. N. Pavlov, E. Sitnikova, A. N. Pisarchik, J. Kurths, and A. E. Hramov, "Statistical properties and predictability of extreme epileptic events," Sci. Rep. **9**, 7243 (2019).
[16]O. N. Pavlova and A. N. Pavlov, "Scaling features of intermittent dynamics: Differences of characterizing correlated and anti-correlated data sets," Physica A **536**, 22586 (2019).
[17]J. F. Muzy, E. Bacry, and A. Arneodo, "The multifractal formalism revisited with wavelets," Int. J. Bifurcation Chaos **4**, 245–302 (1994).
[18]R. M. Bryce and K. B. Sprague, "Revisiting detrended fluctuation analysis," Sci. Rep. **2**, 315 (2012).
[19]K. Hu, P. C. Ivanov, Z. Chen, P. Carpena, and H. E. Stanley, "Effect of trends on detrended fluctuation analysis," Phys. Rev. E **64**, 011114 (2001).
[20]Z. Chen, P. C. Ivanov, K. Hu, and H. E. Stanley, "Effect of nonstationarities on detrended fluctuation analysis," Phys. Rev. E **65**, 041107 (2002).
[21]Y. H. Shao, G. F. Gu, Z. Q. Jiang, W. X. Zhou, and D. Sornette, "Comparing the performance of FA, DFA and DMA using different synthetic long-range correlated time series," Sci. Rep. **2**, 835 (2012).
[22]J. W. Kantelhardt, S. A. Zschiegner, E. Koscielny-Bunde, S. Havlin, A. Bunde, and H. E. Stanley, "Multifractal detrended fluctuation analysis of nonstationary time series," Physica A **316**, 87–114 (2002).
[23]R. Daneman and A. Prat, "The blood-brain barrier," Cold Spring Harb. Perspect. Biol. **7**(1), a020412 (2015).
[24]P. Ballabh, A. Braun, and M. Nedergaard, "The blood-brain barrier: An overview: Structure, regulation, and clinical implications," Neurobiol. Dis. **16**(1), 1–13 (2004).
[25]S. Gupta, S. Dhanda, and R. Sandhir, "Anatomy and physiology of blood-brain barrier," in *Brain Targeted Drug Delivery System* (Elsevier, 2019), pp. 7–31.
[26]J. F. Jordao, C. A. Ayala-Grosso, K. Markham, Y. Huang, R. Chopra, J. McLaurin, K. Hynynen, and I. Aubert, "Antibodies targeted to the brain with image-guided focused ultrasound reduces amyloid-beta plaque load in the TgCRND8 mouse model of Alzheimer's disease," PLoS ONE **5**, e10549 (2010).
[27]G. Leinenga and J. Götz, "Scanning ultrasound removes amyloid-beta and restores memory in an Alzheimer's disease mouse model," Sci. Transl. Med. **7**, 278ra33 (2015).
[28]R. M. Nisbet, A. van der Jeugd, G. Leinenga, H. T. Evans, P. W. Janowicz, and J. Götz, "Combined effects of scanning ultrasound and a tau-specific single chain antibody in a tau transgenic mouse model," Brain **140**, 1220–1230 (2017).

[29]N. E. Fultz, G. Bonmassar, K. Setsompop, R. A. Stickgold, B. R. Rosen, J. R. Polimeni, and L. D. Lewis, "Coupled electrophysiological, hemodynamic, and cerebrospinal fluid oscillations in human sleep," Science **366**, 628–631 (2019).
[30]L. Xie, H. Kang, Q. Xu, M. J. Chen, Y. Liao, M. Thiyagarajan, J. O'Donnell, D. J. Christensen, C. Nicholson, J. J. Iliff, T. Takano, R. Deane, and M. Nedergaard, "Sleep drives metabolite clearance from the adult brain," Science **342**, 373–377 (2013).
[31]S. Da Mesquita, Z. Fu, and J. Kipnis, "The meningeal lymphatic system: A new player in neurophysiology," Neuron **100**, 375–388 (2018).
[32]O. Semyachkina-Glushkovskaya, A. Abdurashitov, A. Dubrovsky, D. Bragin, O. Bragina, N. Shushunova, G. Maslyakova, N. Navolokin, A. Bucharskaya, V. Tuchin, J. Kurths, and A. Shirokov, "Application of optical coherence tomography for in vivo monitoring of the meningeal lymphatic vessels during opening of blood-brain barrier: Mechanisms of brain clearing," J. Biomed. Opt. **22**, 121719 (2017).
[33]O. Semyachkina-Glushkovskaya, V. Chehonin, E. Borisova, I. Fedosov, A. Namykin, A. Abdurashitov, A. Shirokov, B. Khlebtsov, Y. Lyubun, N. Navolokin, M. Ulanova, N. Shushunova, A. Khorovodov, I. Agranovich, A. Bodrova, M. Sagatova, A. E. Shareef, E. Saranceva, T. Iskra, M. Dvoryatkina, E. Zhinchenko, O. Sindeeva, V. Tuchin, and J. Kurths, "Photodynamic opening of the blood-brain barrier and pathways of brain clearing," J. Biophotonics **11**, e201700287 (2018).
[34]O. Semyachkina-Glushkovskaya, D. Postnov, and J. Kurths, "Blood-brain barrier, lymphatic clearance, and recovery: Ariadne's thread in labyrinths of hypotheses," Int. J. Molecular Sci. **19**, 3818 (2018).
[35]Y. Qi, T. Yu, J. Xu, P. Wan, Y. Ma, J. Zhu, Y. Li, H. Gong, Q. Luo, and D. Zhu, "FDISCO: Advanced solvent-based clearing method for imaging whole organs," Sci. Adv. **5**(1), eaau8355 (2019).
[36]H.-L. Wang and T. W. Lai, "Optimization of Evans blue quantitation in limited rat tissue samples," Sci. Rep. **4**, 6588 (2015).
[37]A. Hoffmann, J. Bredno, M. Wendland, N. Derugin, P. Ohara, and M. Wintermark, "High and low molecular weight fluorescein isothiocyanate (FITC)-dextran to assess blood-brain barrier disruption: Technical consideration," Transl. Stroke Res. **2**(1), 106–111 (2011).
[38]N. P. Castellanos and V. A. Makarov, "Recovering EEG brain signals: Artifact suppression with wavelet enhanced independent component analysis," J. Neurosci. Methods **158**, 300–312 (2006).
[39]K. B. Chen, E. Y. Kuo, K. S. Poon, K. S. Cheng, C. S. Chang, Y. C. Liu, and T. W. Lai, "Increase in Evans blue dye extravasation into the brain in the late developmental stage," Neuroreport **23**(12), 699–701 (2012).
[40]D. Fernández-López, J. Faustino, R. Daneman, L. Zhou, S. Y. Lee, N. Derugin, M. F. Wendland, and Z. S. Vexler, "Blood-brain barrier permeability is increased after acute adult stroke but not neonatal stroke in the rat," J. Neurosci. **32**(28), 9588–9600 (2012).